Non-precious metal carbamates as catalysts for the aziridine/CO2 coupling reaction under mild conditions

Non-Precious Metal Carbamates as Catalysts for the Aziridine/CO$_2$ Coupling Reaction Under Mild Conditions

Giulio Bresciani,[a,b] Stefano Zacchini,[b,c] Fabio Marchetti,[a,b] Guido Pampaloni [a,b],*

[a]*Dipartimento di Chimica e Chimica Industriale, University of Pisa, Via G. Moruzzi 13, I-56124*

Pisa, Italy.

[b]*CIRCC, via Celso Ulpiani 27, I-70126 Bari, Italy.*

[c]*Dipartimento di Chimica Industriale "Toso Montanari", University of Bologna, Viale*

Risorgimento 4, I-40136 Bologna, Italy.

* To whom correspondence should be addressed

E-mail address: guido.pampaloni@unipi.it

Abstract

The catalytic potential of a large series of easily available metal carbamates (based on thirteen different non-precious metal elements) was explored for the first time in the coupling reaction between 2-aryl-aziridines and carbon dioxide, working under solventless and ambient conditions and using tetraalkylammonium halides as co-catalysts. The straightforward synthesis of the novel [NbCl$_3$(O$_2$CNEt$_2$)$_2$], **Nb^{Cl}**, and [NbBr$_3$(O$_2$CNEt$_2$)$_2$], **Nb^{Br}**, is reported, and these complexes were fully characterized including by X-ray diffraction. The niobium complex **Nb^{Cl}**, in combination with NBu$_4$I, revealed the best catalyst of the overall series to convert aziridines with small N-alkyl substituents into the corresponding 5-aryl-oxazolidin-2-ones.

Introduction

Carbon dioxide is an inexpensive, largely available, and non-toxic C_1 synthon for organic synthesis and, in this regard, it has received the attention from both academia and industry [1–4]. Despite the high thermodynamic stability and relative kinetic inertness of this molecule [5], CO_2 fixation has been involved in a wide number of processes to obtain valuable chemicals [6–9] such as the synthesis of five-membered cyclic carbamates (2-oxazolidinones). 2-Oxazolidinones are important intermediates in organic chemistry and their core is incorporated in pharmaceutically active substances, such as the antibiotics Linezolid [10] and Tedizolid [11]. Several synthetic strategies to access 2-oxazolidinones have been evaluated making use of CO_2, to be combined with either unsaturated compounds [12–14], amino-alcohols, epoxides [15–17] or aziridines [18–20]. The cycloaddition of carbon dioxide to aziridines is one of the most attractive methods (Scheme 1), and it generally requires both a catalyst and a co-catalyst, acting as Lewis acid and nucleophilic activator, respectively [20,21]. In the last decade, a considerable diversity of catalysts has been investigated to promote this reaction, such as N-heterocyclic compounds [22,23], superbases [24,25], ionic liquids [26], metal complexes [20,27,28], and Metal Organic Frameworks [18,29]. Despite many efforts to overcome the high energy barrier of the aziridine/CO_2 coupling, it is still necessary to work under high pressure of carbon dioxide and/or high temperature conditions [18,22,30–32]. As a matter of fact, environmentally benign catalytic systems working at ambient temperature and pressure are relatively rare [20,27,33].

Scheme 1. General synthesis of 2-oxazolidinone from the aziridine/carbon dioxide coupling (R, R' = alkyl or aryl).
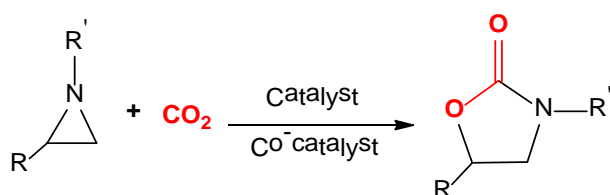
Homoleptic metal N,N-dialkylcarbamates constitute a class of molecular compounds of general formula $[M(O_2CNR_2)_n]_m$, which are typically accessible from the one-pot reaction between an amine and a metal halide precursor under CO_2 atmosphere [34–36] (Equation 1). This synthesis is rather simple and possesses a general character, so that metal carbamates have been prepared for almost all the transition metals and for several main group elements.
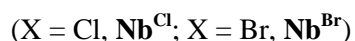
$$MX_n + n\ CO_2 + 2n\ NHR_2 \rightarrow [M(O_2CNR_2)_n] + n\ (NH_2R_2)X \qquad (1)$$

The monoanionic carbamato ligand is relatively robust [37] and, according to the cases, it may act as monodentate, bidentate or bridging, adapting its coordination fashion to the environment and offering the possibility for the generation of vacant coordination site(s). Moreover, it has been demonstrated that the carbamato ligand is prone to exchange its $\{CO_2\}$ fragment with external carbon dioxide, thus enabling CO_2 pre-activation [38,39]. Recently, our group described the use of a range of metal carbamates as active catalysts in carbon dioxide activation reactions, such as the carboxylation of terminal alkynes [40], the cycloaddition to propargyl alcohols [41], and the coupling with epoxides [39,42]. Note that mixed halido-carbamato complexes of high valent metals may provide enhanced catalytic activity compared to the corresponding homoleptic compounds [42,43].

Here, we present a screening study on the use of various metal carbamates, including two unprecedented hybrid niobium(V) halido-carbamates, as catalysts for the reaction between aziridines and CO_2. Tetrabutylammonium halides have been selected as co-catalysts, accordingly to what frequently described in the literature. All the reactions have been conducted under fixed ambient conditions, i.e. room temperature and atmospheric pressure of carbon dioxide, in the light of their favourable incidence in terms of sustainability.

Results and discussion

1) Synthesis of new niobium halido/carbamato complexes

With a view to the possible higher catalytic performance furnished by mixed halido-carbamato complexes (see Introduction), we synthesized the novel Nb^V complexes $[NbCl_3(O_2CNEt_2)_2]$, **Nb^{Cl}**, and $[NbBr_3(O_2CNEt_2)_2]$, **Nb^{Br}**. The synthesis of **Nb^{Cl}** and **Nb^{Br}** is non-classical (compare Eq. 1) and consists in the treatment of the commercial metal pentahalides with sodium carbamate in dichloromethane solution (Eq. 2). The metal products were separated from the side-product sodium chloride by filtration, isolated in 67-85% yields and then fully characterized by elemental analysis, IR and multinuclear NMR spectroscopy.

$$NbX_5 + 2\ NaO_2CNEt_2 \rightarrow [NbX_3(O_2CNEt_2)_2] + 2\ NaCl \qquad (2)$$

$$(X = Cl,\ \mathbf{Nb^{Cl}};\ X = Br,\ \mathbf{Nb^{Br}})$$
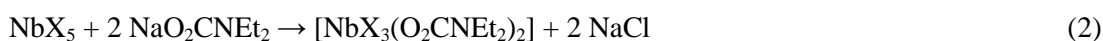
The IR spectra (solid state) of both **Nb^{Cl}** and **Nb^{Br}** display a characteristic intense absorption at ca. 1620 cm^{-1}, ascribable to bidentate carbamato ligands [34,35] and suggesting that the two compounds are isostructural. The NMR spectra (CDCl$_3$ solution) contain a single set of signals; a diagnostic ^{13}C resonance accounting for the bidentate carbamato ligands has been detected at ca. 169 ppm. It should be noted that the ^{13}C resonance related to the carbamato function is very sensitive to the mode of coordination, in that terminal coordination (monodentate carbamate) usually determines a significant upfield shift with respect to bridging coordination (bidentate carbamate) [34,44,45]. For instance, $[Nb(O_2CNMe_2)_5]$ and $[Ta(O_2CNMe_2)_5]$, comprising both monodentate and bidentate ligands, show ^{13}C NMR signals fall at ca. 157 ppm and 166 ppm in both complexes [46]. The ^{93}Nb spectrum of **Nb^{Cl}** exhibits a broad peak centred at -482 ppm [47], whereas a clear ^{93}Nb spectrum could not be recorded for **Nb^{Br}**, presumably due to ligand exchange phenomena [48]. The X-ray molecular structures of **Nb^{Cl}** and **Nb^{Br}** were elucidated by single-crystal X-ray diffraction studies, and views

of the molecules are given in Figures 1 and 2 (oppure 2 in SI). The two compounds are mononuclear, and their common structural motif is in accordance with the spectroscopic features: a niobium(V) centre is coordinated to three halides in a *pseudo-mer* arrangement, and two chelating carbamato ligands. The overall geometry can be described as a pentagonal bipyramid, with the two carbamates and one halide occupying equatorial positions, and the other two halides in apical positions. A search in the Cambridge Crystallographic Data Centre showed that *ca.* 12% of the deposited structures containing niobium display a coordination number of seven, whereas the most common coordination number is six (37% of the entries). The structures of $[NbCl_3(O_2CNEt_2)_2]$ and $[NbBr_3(O_2CNEt_2)_2]$ resemble that previously reported for $[NbCl_3(S_2CNEt_2)_2]$ [49,50], including the mutual *trans* arrangement of the ethyl groups.
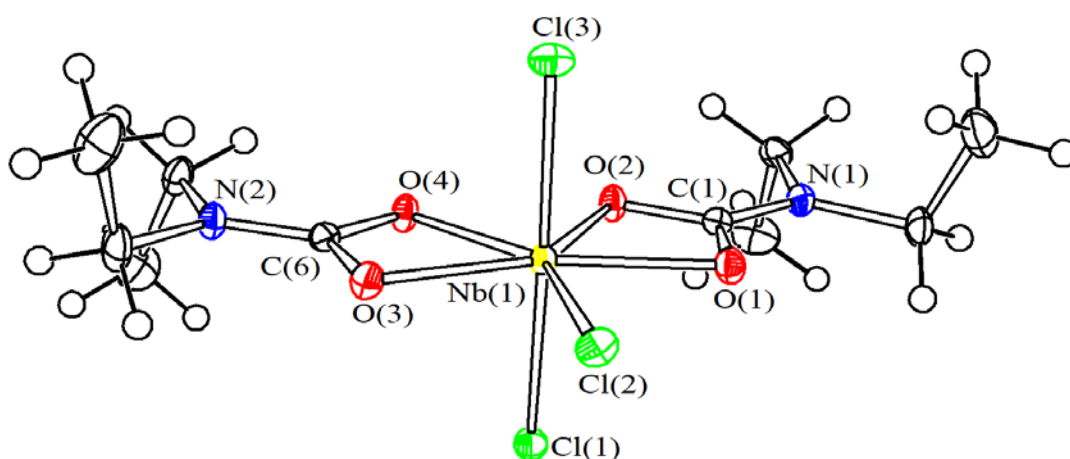
Figure 1. Molecular structure of $[NbCl_3(O_2CNEt_2)_2]$, **Nb**[Cl], with labelling. Displacement ellipsoids are at the 50% probability level. Main bond distances (Å) and angles (°): Nb(1)-Cl(1) 2.3754(5), Nb(1)-Cl(2) 2.3392(5), Nb(1)-Cl(3) 2.3420(5), Nb(1)-O(1) 2.1149(12), Nb(1)-O(2) 2.0802(12), Nb(1)-O(3) 2.0998(12), Nb(1)-O(4) 2.0764(11), C(1)-O(1) 1.300(2), C(1)-O(2) 1.3016(19), C(1)-N(1) 1.309(2), C(6)-O(3) 1.303(2), C(6)-O(4) 1.299(2), C(6)-N(2) 1.309(2), O(1)-Nb(1)-O(2) 62.46(4), O(3)-Nb(1)-O(4) 62.72(4), Cl(1)-Nb(1)-Cl(3) 175.146(16), Cl(1)-Nb(1)-Cl(2) 91.391(15), Cl(2)-Nb(1)-Cl(3) 93.461(16), O(1)-C(1)-O(2) 113.47(14), O(3)-C(6)-O(4) 113.29(14), sum at C(1) 360.0(2), sum at C(6) 360.0(2), sum at N(1) 360.0(2), sum at N(2) 360.0(2).
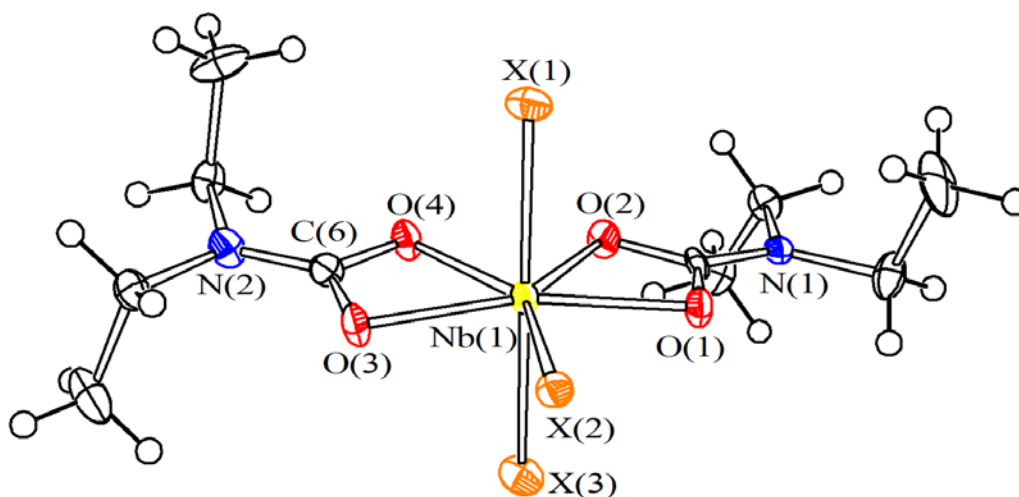
Figure 2. Molecular structure of [NbX$_3$(O$_2$CNEt$_2$)$_2$], **Nb^{Br}**, with labelling. Displacement ellipsoids are at the 50% probability level. Displacement ellipsoids are at the 50% probability level. The positions labelled X(1), X(2) and X(3) are disordered Br/Cl. Main bond distances (Å) and angles (°): Nb(1)-X(1) 2.4637(16), Nb(1)-X(2) 2.4726(17), Nb(1)-X(3) 2.5017(15), Nb(1)-O(1) 2.111(7), Nb(1)-O(2) 2.077(70), Nb(1)-O(3) 2.104(7), Nb(1)-O(4) 2.085(7), C(1)-O(1) 1.302(12), C(1)-O(2) 1.288(12), C(1)-N(1) 1.306(13), C(6)-O(3) 1.293(13), C(6)-O(4) 1.307(13), C(6)-N(2) 1.298(12), O(1)-Nb(1)-O(2) 62.0(3), O(3)-Nb(1)-O(4) 62.7(3), X(1)-Nb(1)-X(3) 176.63(6), X(1)-Nb(1)-X(2) 90.54(5), X(2)-Nb(1)-X(3) 92.75(5), O(1)-C(1)-O(2) 112.8(8), O(3)-C(6)-O(4) 114.0(8), sum at C(1) 360.0(16), sum at C(6) 360.0(16), sum at N(1) 359.7(15), sum at N(2) 360.0(15).

Besides the unprecedented **Nb^{Cl}** and **Nb^{Br}**, a large selection of known metal carbamates has been investigated in the present work, including homoleptic compounds of group 4 and 5 metals, iron, cobalt, copper, silver, and main group elements (Al, Sn, Si), and mixed species with halido and/or oxido co-ligands of titanium(III), niobium(V) and tungsten(VI). The structures of these compounds are represented in Figure 3.
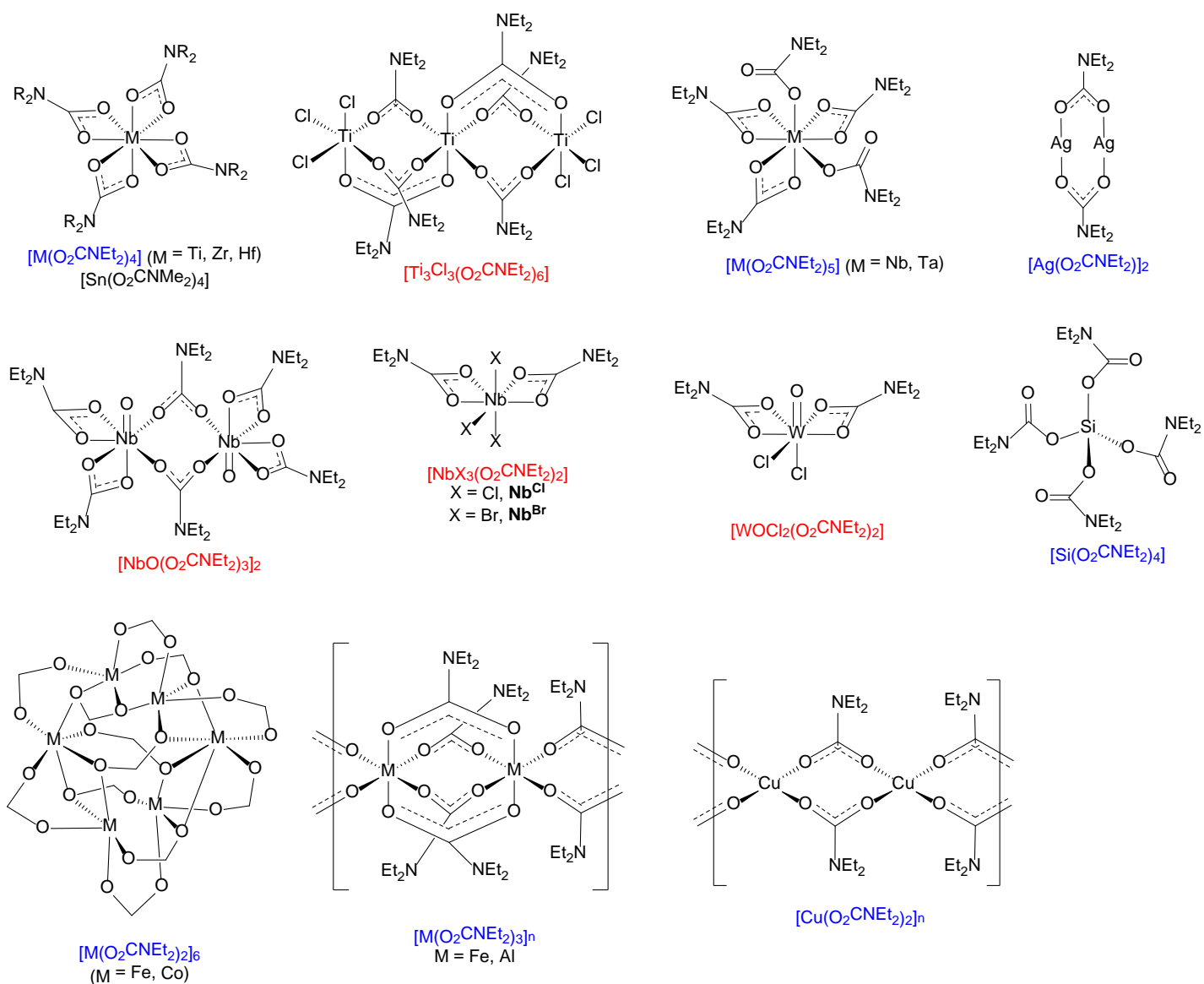
Figure 3. Structures of metal carbamates investigated in this work (blue: homoleptic compounds; red: mixed-ligand compounds). $[M(O_2CNEt_2)_3]_n$ (M = Fe, Al) and $[Cu(O_2CNEt_2)_2]_n$ are polymeric materials.

2) Catalytic studies

First, we tested the catalytic activity of carbamato complexes (see Figure 3) in the coupling reaction of 1-methyl-2-phenylaziridine, which was selected as a model substrate, with carbon dioxide from a balloon, in the absence of solvent. The systems were maintained at room temperature (ca. 25 °C) for 24 hours, and tetrabutylammonium bromide (TBAB) was employed as a co-catalyst. The results of this preliminary study are reported in **Table 1**.

Table 1. Conversion of 1-methyl-2-phenylaziridine into 3-methyl-5-phenyloxazolidin-2-one: effect of the catalyst.
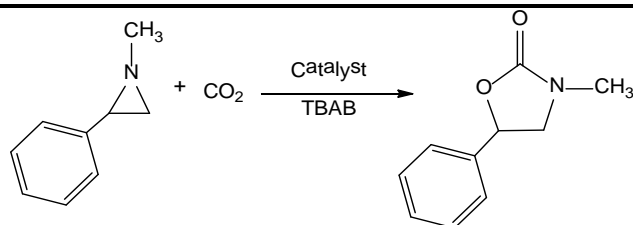
Entry	Catalyst	Yield%
1	$[Ti(O_2CNEt_2)_4]$	5
2	$[TiCl_2(O_2CNEt_2)_2]$	61
3	$[Zr(O_2CNEt_2)_4]$	47
4	$[Hf(O_2CNEt_2)_4]$	19
5	$[Nb(O_2CNEt_2)_5]$	41
6	$[NbO(O_2CNEt_2)_3]$	14
7	$[NbCl_3(O_2CNEt_2)_2]$ (**Nb^{Cl}**)	68
8	$[NbBr_3(O_2CNEt_2)_2]$ (**Nb^{Br}**)	61
9	$[Ta(O_2CNEt_2)_5]$	66
10	$[WOCl_2(O_2CNEt_2)_2]$	33
11	$[Fe(O_2CNEt_2)_2]$	13
12	$[Fe(O_2CNEt_2)_3]$	5
13	$[Co(O_2CNEt_2)_2]$	4
14	$[Cu(O_2CNEt_2)_2]$	4
15	$[Ag(O_2CNEt_2)]$	4
16	$[Al(O_2CNEt_2)_3]$	Traces
17	$[Si(O_2CNEt_2)_4]$	61
18	$[Sn(O_2CNMe_2)_4]$	65

Reaction conditions: Aziridine 1.0 mmol, Catalyst 1 mol%, co-catalyst $[NBu_4]Br$ 5 mol%, T = 25 °C, pCO_2 = 1 atm, t = 24 h. Yield determined by ^1H NMR using 1,1,2,2-tetrachloroethane as standard.

It can be observed that late transition metal carbamates and the aluminium species are not suitable to promote the examined reaction. Complicated mixtures of products were obtained in low amounts from $[Fe(O_2CNEt_2)_2]$, $[Fe(O_2CNEt_2)_3]$ and $[Ag(O_2CNEt_2)]$, presumably including low molecular oligomers of polyamine, poly(urethane-amine) and piperazines [51,52].

On the other hand, 3-methyl-5-phenyloxazolidin-2-one was selectively generated in moderate to good yields when some specific high valent metal complexes were employed. The Ta^V homoleptic carbamate and the hybrid chlorido-carbamato complexes of Ti^{IV} and Nb^V revealed effective (61-

68% yields). Moreover, a comparable performance was exhibited by $[Si(O_2CNEt_2)_4]$ and $[Sn(O_2CNMe_2)_4]$. Interestingly, no traces of the other possible regioisomer, 3-methyl-4-phenyloxazolidin-2-one, were detected in the final mixtures. In alignment with what previously observed in other catalytic processes (see Introduction), halido-carbamato complexes exhibit a superior activity with respect to their homoleptic counterparts (compare runs 5 with 7 and 8 and run 1 with 2). This feature might be explained based on a less steric hindrance around the metal centre in the non-homoleptic species, favouring the coordination of the substrate and thus accelerating the reaction. It must be noted that this is the first time that compounds based on titanium, tantalum, tungsten, silicon and tin are investigated as possible catalysts for the aziridine/CO_2 coupling reaction.

Following the preliminary screening and adopting the same reaction conditions in terms of time, CO_2 pressure and temperature, a selection of active catalytic precursors was further investigated in combination with different tetrabutylammonium halides (**Table 2**). The selected catalysts are good candidates in view of a sustainable process, being based on earth-abundant elements (Si or Sn) or nontoxic transition metals (Nb, Ta) [53]. It was confirmed that 5% molar concentration of tetrabutylammonium bromide (TBAB) is necessary to achieve satisfying yields of product, using $[Si(O_2CNEt_2)_4]$ and $[Sn(O_2CNMe_2)_4]$. On the other hand, these latter catalysts revealed much less performing when combined with tetrabutylammonium chloride (TBAC) or tetrabutylammonium iodide (TBAI).

Among the transition metal compounds, the hybrid complex **Nb^{Cl}** worked as the best catalyst. It was tested in combination with the three tetraalkylammonium salts (Table 2, runs 14-16), with the idea in mind that the possible exchange between the chloride ligand and the external halide source [54] might induce favourable reaction pathways. As a matter of fact, TBAB and TBAC afforded comparable yields (ca. 70%) of the oxazolidinone, and TBAI provided a better result (86% yield).

Table 2. Catalytic conversion of 1-methyl-2-phenylaziridine into 3-methyl-5-phenyloxazolidin-2-one: effect of the co-catalyst.
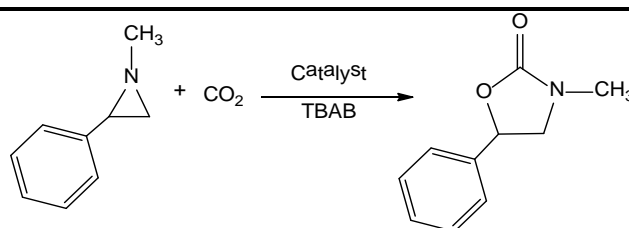
Entry	Catalyst	Co-Catalyst (mol%)	Yield%
1	$[Si(O_2CNEt_2)_4]$	$[NBu_4]Cl$ (5)	Traces
2	$[Si(O_2CNEt_2)_4]$	$[NBu_4]Cl$ (2)	4
3	$[Si(O_2CNEt_2)_4]$	$[NBu_4]Br$ (5)	61
4	$[Si(O_2CNEt_2)_4]$	$[NBu_4]Br$ (2)	41
5	$[Si(O_2CNEt_2)_4]$	$[NBu_4]I$ (5)	5
6	$[Si(O_2CNEt_2)_4]$	$[NBu_4]I$ (2)	3
7	$[Sn(O_2CNMe_2)_4]$	$[NBu_4]Cl$ (5)	Traces
8	$[Sn(O_2CNMe_2)_4]$	$[NBu_4]Cl$ (2)	4
9	$[Sn(O_2CNMe_2)_4]$	$[NBu_4]Br$ (5)	65
10	$[Sn(O_2CNMe_2)_4]$	$[NBu_4]Br$ (2)	47
11	$[Sn(O_2CNMe_2)_4]$	$[NBu_4]I$ (5)	2
12	$[Sn(O_2CNMe_2)_4]$	$[NBu_4]I$ (2)	3
13	$[NbCl_3(O_2CNEt_2)_2]$ ($\mathbf{Nb^{Cl}}$)	$[NBu_4]Br$ (5)	68
14	$\mathbf{Nb^{Cl}}$	$[NBu_4]Br$ (2)	58
15	$\mathbf{Nb^{Cl}}$	$[NBu_4]Cl$ (5)	70
16	$\mathbf{Nb^{Cl}}$	$[NBu_4]I$ (5)	86
17	$[NbBr_3(O_2CNEt_2)_2]$ ($\mathbf{Nb^{Br}}$)	$[NBu_4]Br$ (5)	61
18	$\mathbf{Nb^{Br}}$	$[NBu_4]I$ (5)	53
19	$[Ta(O_2CNEt_2)_5]$	$[NBu_4]Br$ (5)	66
20	$[Ta(O_2CNEt_2)_5]$	$[NBu_4]I$ (5)	Traces

Reaction conditions: Aziridine 1.0 mmol, Catalyst 1 mol%, T = 25 °C, pCO_2 = 1 atm, t = 24 h. Yields determined by ^{1}H NMR using 1,1,2,2-tetrachloroethane as standard.

According to the outcomes reported in **Table 2**, $[NbCl_3(O_2CNEt_2)_2]$ ($\mathbf{Nb^{Cl}}$), $[Si(O_2CNEt_2)_4]$ and $[Sn(O_2CNMe_2)_4]$, in combination with the respective optimal co-catalyst, were explored for their activity in the coupling of carbon dioxide with two other 1-alkyl-2-phenyl-aziridines (**Table 3**, runs 4-10). The catalytic system $\mathbf{Nb^{Cl}}$/TBAI emerged as the most performing to convert 1-ethyl-2-phenylaziridine into the corresponding oxazolidinone in a regiospecific manner. Otherwise, the presence of an isopropyl N-substituent prevented the coupling process under the employed mild

conditions; some unfavourable impact of the size of the nitrogen substituent on the formation of five-membered oxazolidinones via CO_2 fixation was previously documented [19,23,30]. The **Nb**[**Cl**]/TBAI combination was successfully employed to extend the synthesis to 3-methyl(ethyl)-5-aryloxazolidin-2-ones bearing different para-substituents on the aryl ring (**Table 3**, runs 11-15).

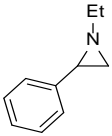**Table 3.** Catalytic conversion of 1-alkyl-2-arylaziridines into 3-alkyl-5-aryloxazolidin-2-ones.
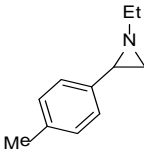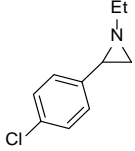
Entry	X	R	Catalyst	Co-catalyst	Yield %
1	H	Me	[Si(O₂CNEt₂)₄]	[NBu₄]Br	61
2	H	Me	[Sn(O₂CNMe₂)₄]	[NBu₄]Br	65
3	H	Me	[NbCl₃(O₂CNEt₂)₂] (**Nb**[**Cl**])	[NBu₄]I	86
4	H	Et	[Si(O₂CNEt₂)₄]	[NBu₄]Br	31
5	H	Et	[Sn(O₂CNMe₂)₄]	[NBu₄]Br	34
6	H	Et	**Nb**[**Cl**]	[NBu₄]I	53
7	H	ᶦPr	[Si(O₂CNEt₂)₄]	[NBu₄]Br	Traces
8	H	ᶦPr	[Sn(O₂CNMe₂)₄]	[NBu₄]Br	Traces
9	H	ᶦPr	**Nb**[**Cl**]	[NBu₄]Br	Traces
10	H	ᶦPr	**Nb**[**Cl**]	[NBu₄]I	5
11	Me	Me	**Nb**[**Cl**]	[NBu₄]I	50
12	Me	Et	**Nb**[**Cl**]	[NBu₄]I	41
13	Cl	Me	**Nb**[**Cl**]	[NBu₄]I	58
14	Cl	Et	**Nb**[**Cl**]	[NBu₄]I	49
15	F	Me	**Nb**[**Cl**]	[NBu₄]I	56

Reaction conditions: Aziridine 1.0 mmol, Catalyst 1 mol%, Co-catalyst 5 mol%, T = 25 °C, pCO_2 = 1 atm, t = 24 h. Yields determined by ¹H NMR using 1,1,2,2-tetrachloroethane as standard.

Note that the straightforward synthesis of 3-methyl-5-aryloxazolidinones from aziridines under sustainable conditions is not a trivial task, and actually more expensive and elaborated catalytic systems, as well as more drastic experimental conditions, have been often reported to access the

same products as those efficiently obtained here. Selected examples from the literature since 2018 are compiled in Table 4. The preparation of 5-(4-fluorophenyl)-3-methyloxazolidin-2-one via aziridine/CO_2 coupling is unprecedented.

Table 4. Selection of data from the literature for the coupling between carbon dioxide and 2-arylaziridines with N-methyl/ethyl substituents, affording 5-aryl-2-oxazolidinones.

Aziridine	Catalyst / cocatalyst	T (°C)	p CO_2 (atm)	Reaction time (h)	Yield (%)	Ref.
	Ru^{VI} imidoporphyrin complex / NBu$_4$Cl	100	6	6	65	[31]
	carbodicarbene (CDC)	80	20	12	75	[22]
	Di-europium complex / DBU	50	1	48	83	[20]

Conclusions

Metal carbamates are easily available and cost-effective compounds which possess the ability to dynamically activate carbon dioxide, and for this reason have been successfully employed as homogeneous catalytic precursors in some CO_2 activation reactions. Herein, we describe a study aimed to assess the potential of carbamates of a vast range of metal elements in the widely investigated coupling reaction of aziridines with carbon dioxide affording five-membered cyclic carbamates. A newly synthesized mononuclear niobium(V) mixed chlorido-carbamato complex revealed the most active catalyst in combination with tetrabutylammonium iodide, confirming the previously observed tendency that non-homoleptic carbamates based on high valent metals possess a superior catalytic potential compared to the corresponding homoleptic species. The regiospecific synthesis of 3-alkyl-5-aryloxazolidin-2-ones was achieved in good yields from 2-aryl-aziridines

with small N-groups (methyl or ethyl). This process is featured by environmentally benign conditions, i.e. the use of simple catalysts based on earth-abundant and/or non-toxic elements, atmospheric pressure of carbon dioxide and room temperature. Remarkably, the syntheses of some of the products here obtained have been recently described according to the same reaction (aziridine/CO_2 coupling), but usually require drastic experimental conditions and/or more elaborated catalytic systems, and are sometimes non-regioselective [20,22,55,56]. On the other hand, the steric hindrance of the aziridine is a limiting factor with reference to the present catalytic systems, since a bulkier group on the nitrogen atom prevents the formation of the related oxazolidinone.

Experimental

1) Materials and methods.

Operations were conducted under N_2 atmosphere using standard Schlenk techniques; the reaction vessels were oven-dried at 140 °C prior to use, evacuated (10^{-2} mmHg) and then filled with N_2. Carbon dioxide (99.99%) was purchased from Rivoira, while organic reactants (TCI Europe, Merck or Strem) were commercial products of the highest purity available, stored under N_2 atmosphere as received. Solvents (Merck) were distilled before use over appropriate drying agents. Compounds NaO_2CNEt_2 [57], $[M(O_2CNEt_2)_4]$ (M = Ti, Zr, Hf) [58], $[TiCl_2(O_2CNEt_2)_2]$ [44], $[M(O_2CNEt_2)_5]$ (M = Nb, Ta) [59], $[NbO(O_2CNEt_2)_3]$ [60], $[WOCl_2(O_2CNEt_2)_2]$ [57], $[Fe(O_2CNEt_2)_2]$ [61], $[Fe(O_2CNEt_2)_3]$ [62], $[Co(O_2CNEt_2)_2]$ [63], $[Cu(O_2CNEt_2)_2]$ [64], $[Ag(O_2CNEt_2)]$ [65], $[Al(O_2CNEt_2)_3]$ [42], $[Si(O_2CNEt_2)_4]$ [66], $[Sn(O_2CNEt_2)_4]$ [67] and 2-arylaziridines [26] were prepared according to literature procedures. IR spectra (650-4000 cm^{-1}) were recorded on a Perkin Elmer Spectrum One FT-IR spectrometer, equipped with a UATR sampling accessory. NMR spectra were recorded at 298 K with a Bruker Avance II DRX 400 instrument equipped with a BBFO broadband probe. [1]H chemical shifts (expressed in ppm) were referenced to the residual solvent peaks [68] while chemical shifts for [93]Nb were referenced to external $[NEt_4]NbCl_6$. Yields of oxazolidinones were evaluated on ^{1}H NMR spectra using 1,1,2,2-tetrachloroethane as internal standard. CHN analyses were performed on a Vario MICRO cube instrument (Elementar). The halide content was determined by the Volhard method [69], by dissolving the solid samples in aqueous KOH at boiling temperature, followed by cooling to room temperature and addition of HNO_3 up to acidic pH.

2) Synthesis and characterization of $[NbX_3(O_2CNEt_2)_2]$ (X = Cl, Nb^{Cl}; X = Br, Nb^{Br})

The preparation of Nb^{Cl} is described in detail; Nb^{Br} was prepared using an analogous procedure.

$[NbCl_3(O_2CNEt_2)_2]$. A suspension of $NbCl_5$ (370 mg, 1.37 mmol) in CH_2Cl_2 (30 mL) was treated with NaO_2CNEt_2 (390 mg, 2.80 mmol). The mixture was stirring for 20 hours at room temperature, then the resulting precipitate (NaCl) was filtered off. The solvent was evaporated under vacuum,

and the residue was added of THF (10 mL). The tetrahydrofuran solution was treated with hexane (30 mL), and the mixture was cooled to ca. −30 °C. The obtained suspension was filtered, and the solid was dried under vacuum affording $\mathbf{Nb^{Cl}}$ (0.50 g, 85% yield) as a moisture-sensitive yellow microcrystalline solid. Anal. Calc. for $C_{10}H_{20}Cl_3N_2NbO_4$: C, 27.8; H, 4.7; N, 6.5; Cl, 24.6. Found: C, 28.0; H, 4.6; N, 6.6 %; Cl, 24.3. IR (solid state): $\tilde{\upsilon}/cm^{-1}$ = 2977w, 2942w, 1616vs (C=O), 1443w, 1410m, 1382w-m, 1310m, 1261w-m, 1197w-m, 1089m, 1020w-m, 979w, 839s, 799m, 776m-s. ^1H NMR (CDCl$_3$): δ/ppm = 3.59 (q, 2H, $^3J_{HH}$ = 7.2 Hz, CH$_2$); 1.30 (t, 3H, $^3J_{HH}$ = 7.0 Hz, CH$_3$). $^{13}C\{^1H\}$ NMR (CDCl$_3$): δ/ppm = 168.7 (C=O); 40.3 (CH$_2$); 13.8 (CH$_3$). $^{93}Nb\{^1H\}$ (CDCl$_3$): δ/ppm = − 482 (s, $\Delta\nu_{1/2}$ = 6·10^3 Hz). Crystals suitable for X-ray analysis were obtained from a THF solution of **5** layered with hexane and stored at −30°C for 5 days.

[NbBr$_3$(O$_2$CNEt$_2$)$_2$], Nb^{Br}. Highly moisture sensitive dark-red solid, 67% yield from NbBr$_5$ (390 mg, 0.79 mmol) and NaO$_2$CNEt$_2$ (220 mg, 1.58 mmol). Anal. Calc. for $C_{10}H_{20}Br_3N_2NbO_4$: C, 21.3; H, 3.6; N, 5.0; Br, 42.4. Found: C, 21.5; H, 3.5; N, 5.1; Br, 42.1. IR (solid state): $\tilde{\upsilon}/cm^{-1}$ = 2975w, 2934w, 1706w-m, 1621m-s (C=O), 1569s, 1443m-s, 1380s, 1314s-sh, 1260m, 1200m, 1097w-m, 1074m-s, 976w-m, 944vw, 838m, 793m-s. ^1H NMR (CDCl$_3$): δ/ppm = 3.61 (m, 2H, CH$_2$); 1.33 (m, 3H, CH$_3$). $^{13}C\{^1H\}$ NMR (CDCl$_3$): δ/ppm = 168.7 (C=O); 40.5 (CH$_2$); 14.0 (CH$_3$) ppm. Crystals suitable for X-ray analysis were obtained from a THF solution of $\mathbf{Nb^{Br}}$ layered with hexane and stored at −30°C for 5 days.

3) X-ray crystallography

Crystals of $\mathbf{Nb^{Cl}}$ and $\mathbf{Nb^{Br}}$ suitable for X-ray analysis were collected from the respective THF solutions layered with hexane (THF/hexane ratio 1:3). Crystal data and collection details are reported in Table 4. Data were recorded on a Bruker APEX II diffractometer equipped with a PHOTON100 detector using Mo–Kα radiation. Data were corrected for Lorentz polarization and absorption effects (empirical absorption correction SADABS) [70]. The structures were solved by

direct methods and refined by full-matrix least-squares based on all data using F^2 [71]. Hydrogen atoms were fixed at calculated positions and refined by a riding model. All non-hydrogen atoms were refined with anisotropic displacement parameters. The crystals of **6** are racemically twinned with refined Flack parameter 0.35(2) [72]. Within the structure of **Nb^{Br}**, the positions of the halide ligands are actually disordered Br/Cl. These haves been refined applying dummy atom constraints (EADP and EXYZ lines in SHLEXL) resulting in the following refined occupancy factor: X(1) = 0.703(9) Br and 0.397(9) Cl; X(2) = 0.577(10) Br and 0.423(9) Cl; X(3) = 0.769(9) Br and 0.231(9) Cl.

Table 4. Crystal data and measurement details for [NbCl$_3$(O$_2$CNEt$_2$)$_2$] (**Nb^{Cl}**) and [NbBr$_3$(O$_2$CNEt$_2$)$_2$] (**Nb^{Br}**).

	Nb^{Cl}	Nb^{Br}
Formula	C$_{10}$H$_{20}$Cl$_3$N$_2$NbO$_4$	C$_{10}$H$_{20}$Br$_{2.06}$Cl$_{0.94}$N$_2$NbO$_4$
FW	431.54	522.90
T, K	100(2)	100(2)
λ, Å	0.71073	0.71073
Crystal system	Monoclinic	Monoclinic
Space group	$P2_1/c$	$P2_1$
a, Å	15.3038(15)	7.4915(14)
b, Å	16.5965(16)	12.296(2)
c, Å	13.8932(14)	9.6832(18)
β,°	90.886(2)	95.837(8)
Cell Volume, Å^3	3528.3(6)	887.4(3)
Z	8	2
D_c, g·cm^{-3}	1.625	1.957
μ, mm^{-1}	1.147	5.458
F(000)	1744	510
Crystal size, mm	0.25×0.21×0.14	0.22×0.16×0.12
θ limits,°	1.331-28.999	2.114-26.000
Reflections collected	56714	8480
Independent reflections	9373 [R_{int} = 0.0376]	3474 [R_{int} = 0.0625]
Data / restraints /parameters	9373 / 0 / 369	3474 / 1 / 185
Goodness on fit on F^2	1.089	1.018
R_1 ($I > 2\sigma(I)$)	0.0259	0.0427
wR_2 (all data)	0.0553	0.0940
Largest diff. peak and hole, e Å^{-3}	0.380 / –0.600	1.368 / –0.998

4) Reactions between 2-aryl-aziridines and carbon dioxide.

a) General details. The appropriate amounts of catalyst and co-catalyst were introduced into a Schlenk tube. The tube was evacuated with a vacuum pump and then filled with CO_2. The vacuum/CO_2 sequence was repeated twice. Under a stream of carbon dioxide, the selected aziridine (1 mmol) was added, and the resulting mixture was stirred for 24 hours at room temperature under atmospheric pressure of CO_2 from a balloon. An exact amount of 1,1,2,2-tetrachloroethane (0.2 mL) was added, and an aliquot (ca 0.1 mL) of the mixture was mixed with $CDCl_3$ (0.5 mL) in an NMR tube. Yields were determined by ^{1}H NMR spectroscopy using 1,1,2,2-tetrachloroethane as internal standard.

b) NMR characterization of organic products

1-methyl-2-phenylaziridine. Colourless liquid. ^{1}H NMR ($CDCl_3$): δ/ppm = 7.37–7.21 (m, 5H, Ph), 2.50 (s, 3H, NMe), 2.28 (m, 1H, CH), 1.91 (d, $^3J_{HH}$ = 3.2 Hz, 1H, CH_2), 1.63 (d, $^3J_{HH}$ = 6.7 Hz, 1H, CH_2).

1-ethyl-2-phenylaziridine. Colourless liquid. ^{1}H NMR ($CDCl_3$): δ/ppm = 7.40–7.24 (m, 5H, Ph), 2.53–2.44 (m, 2H, NCH_2), 2.34 (m, 1H, CH), 1.94 (d, $^3J_{HH}$ = 3.2 Hz, 1H, CH_2), 1.68 (d, $^3J_{HH}$ = 6.7 Hz, 1H, CH_2), 1.26 (t, $^3J_{HH}$ = 7.2 Hz, 3H, CH_3).

1-isopropyl-2-phenylaziridine. Colourless liquid. ^{1}H NMR ($CDCl_3$): δ/ppm = 7.35–7.24 (m, 5H, Ph), 2.40 (dd, $^3J_{HH}$ = 3.3 Hz, 3H, NMe), 1.95, 1.71 (d, $^3J_{HH}$ = 3.2 Hz, 1H, CH_2), 1.67 (m, $^3J_{HH}$ = 6.2 Hz, 1H, CH^{iPr}), 1.26, 1.24 (d, $^3J_{HH}$ = 6.3 Hz, 6H, CH_3^{iPr}).

1-methyl-2-(p-tolyl)aziridine. Colourless liquid. ^{1}H NMR ($CDCl_3$): δ/ppm = 7.16 (m, 4H, C_6H_4); 2.52 (s, 3H, NMe); 2.37 (s, 3H, C_6H_4Me); 2.28 (m, 1H, CH); 1.92 (d, $^3J_{HH}$ = 3.2 Hz, 1H, CH_2); 1.63 (d, $^3J_{HH}$ = 6.7 Hz, 1H, CH_2).

1-ethyl-2-(p-tolyl)aziridine. Colourless liquid. ^{1}H NMR ($CDCl_3$): δ/ppm = 7.18 (m, 4H, C_6H_4); 2.55–2.43 (m, 2H, NCH_2); 2.38 (s, 3H, C_6H_4Me); 2.32 (m, 1H, CH); 1.92 (m, 1H, CH_2); 1.67 (d, $^3J_{HH}$ = 6.7 Hz, 1H, CH_2); 1.26 (t, $^3J_{HH}$ = 7.2 Hz, 3H, CH_3).

1-methyl-2-(4-chlorophenyl)aziridine. Colourless liquid. ^{1}H NMR (CDCl$_3$): δ/ppm = 7.27–7.14 (m, 4H, C$_6$H$_4$); 2.48 (s, 3H, NMe); 2.24 (m, 1H, CH); 1.85 (d, 1H, CH$_2$, ^{3}J$_{HH}$ = 3.0); 1.63 (d, 1H, CH$_2$, ^{3}J$_{HH}$ = 6.7).

1-ethyl-2-(4-chlorophenyl)aziridine. Colourless liquid. ^{1}H NMR (CDCl$_3$): δ/ppm = 7.28–7.18 (m, 4H, C$_6$H$_4$); 2.45 (m, 2H, NCH$_2$); 2.29 (m, 1H, CH); 1.86 (d, ^{3}J$_{HH}$ = 3.2, 1H, CH$_2$); 1.68 (d, ^{3}J$_{HH}$ = 6.7 Hz, 1H, CH$_2$,); 1.21 (t, ^{3}J$_{HH}$ = 7.2 Hz, 3H, CH$_3$).

1-methyl-2-(4-fluorophenyl)aziridine. Colourless liquid. ^{1}H NMR (CDCl$_3$): δ/ppm = 7.17, 6.97 (m, 4H, C$_6$H$_4$); 2.47 (s, 3H, NMe); 2.24 (m, 1H, CH); 1.84 (d, 1H, CH$_2$, ^{3}J$_{HH}$ = 3.4); 1.60 (d, 1H, CH$_2$, ^{3}J$_{HH}$ = 6.6).

c) NMR characterization of 5-phenyl-oxazolidin-2-ones

3-methyl-5-phenyloxazolidin-2-one [26,73]. ^{1}H NMR (CDCl$_3$): δ/ppm = 7.41–7.26 (m, 5H, Ph); 5.48 (t, ^{3}J$_{HH}$ = 8.6 Hz, 1H, CH); 3.91, 3.44 (t, ^{3}J$_{HH}$ = 8.6 Hz, 2H, CH$_2$); 2.92 (s, 3H, CH$_3$).

3-ethyl-5-phenyloxazolidin-2-one [26,73]. ^{1}H NMR (CDCl$_3$): δ/ppm = 7.29–7.20 (m, 5H, Ph); 5.33 (t, ^{3}J$_{HH}$ = 8.7 Hz, 1H, CH); 3.80 (t, ^{3}J$_{HH}$ = 8.7 Hz, 1H, CH$_2$); 3.30-3.15 (m, 3H, CH$_2$ + NCH$_2$); 1.04 (t, ^{3}J$_{HH}$ = 7.2 Hz, 3H, CH$_3$).

3-isopropyl-5-phenyloxazolidin-2-one [26,73]. ^{1}H NMR (CDCl$_3$): δ/ppm = 7.38–7.28 (m, 5H, Ph); 5.43 (t, 1H, ^{3}J$_{HH}$ = 8.4 Hz, CH); 4.12 (m, 1H, CH^{iPr}); 3.84, 3.33 (t, ^{3}J$_{HH}$ = 8.6 Hz, 2H, CH$_2$); 1.18, 1.12 (d, ^{3}J$_{HH}$ = 6.6 Hz, 6H, CH$_3$^{iPr})

3-methyl-5-(p-tolyl)oxazolidin-2-one [28,73]. ^{1}H NMR (CDCl$_3$): δ/ppm = 7.27-7.21 (m, 4H, C$_6$H$_4$); 5.46 (t, ^{3}J$_{HH}$ = 8.4 Hz, 1H, CH); 3.90, 3.45 (t, ^{3}J$_{HH}$ = 8.4 Hz, 2H, CH$_2$), 2.94 (s, 3H, NCH$_3$); 2.38 (s, 3H, C$_6$H$_4$C*H*$_3$) ppm.

3-ethyl-5-(p-tolyl)oxazolidin-2-one [26,73]. ^{1}H NMR (CDCl$_3$): δ/ppm = 7.20-7.13 (m, 4H, C$_6$H$_4$); 5.39 (t, ^{3}J$_{HH}$ = 8.3 Hz, 1H, CH), 3.83 (t, ^{3}J$_{HH}$ = 8.6 Hz, 1H, CH$_2$), 3.38-3.25 (m, 3H, CH$_2$ + NCH$_2$), 2.30 (s, 3H, C$_6$H$_4$C*H*$_3$), 1.12 (t, ^{3}J$_{HH}$ = 7.3 Hz, 3H, CH$_2$C*H*$_3$) ppm.

5-(4-chlorophenyl)-3-methyloxazolidin-2-one [28,73]. ^1H NMR (CDCl$_3$): δ/ppm = 7.38-7.28 (m, 4H, C$_6$H$_4$); 5.45 (t, $^3J_{HH}$ = 8.3 Hz, 1H, CH); 3.91, 3.40 (t, $^3J_{HH}$ = 8.3 Hz, 2H, CH$_2$); 2.92 (s, 3H, CH$_3$) ppm

5-(4-chlorophenyl)-3-ethyloxazolidin-2-one [26,73]. ^1H NMR (CDCl$_3$): δ/ppm = 7.37, 7.29 (d, $^3J_{HH}$ = 7.9 Hz, 4H, C$_6$H$_4$); 5.45 (t, $^3J_{HH}$ = 8.3 Hz, 1H, CH); 3.92 (t, $^3J_{HH}$ = 8.3 Hz, 1H, CH$_2$); 3.44-3.30 (m, 3H, CH$_2$ + NCH$_2$); 1.17 (t, $^3J_{HH}$ = 7.3 Hz, 3H, CH$_3$) ppm

5-(4-fluorophenyl)-3-methyloxazolidin-2-one [73]. ^1H NMR (CDCl$_3$): δ/ppm = 7.36-7.32, 7.11-7.07 (m, 4H, C$_6$H$_4$); 5.46 (t, $^3J_{HH}$ = 8.1 Hz, 1H, CH); 3.90, 3.42 (t, $^3J_{HH}$ = 8.4 Hz, 2H, CH$_2$); 2.93 (s, 3H, CH$_3$) ppm.

Acknowledgements

Supporting Information Available

NMR and IR spectra of new niobium complexes and of organic compounds. CCDC reference numbers 2062321 (**Nb^{Cl}**) and 2062322 (**Nb^{Br}**) contain the supplementary crystallographic data for the X-ray studies reported in this paper. These data can be obtained free of charge at www.ccdc.cam.ac.uk/conts/retrieving.html (or from the Cambridge Crystallographic Data Centre, 12, Union Road, Cambridge CB2 1EZ, UK; fax: (internat.) +44-1223/336-033; e-mail: deposit@ccdc.cam.ac.uk).

References

1   E. Furimsky, *Ind. Eng. Chem. Res.*, 2020, **59**, 15393–15423.

2   M. Aresta, A. Dibenedetto and A. Angelini, *Chem. Rev.*, 2014, **114**, 1709–1742.

3   W. Zhou, K. Cheng, J. Kang, C. Zhou, V. Subramanian, Q. Zhang and Y. Wang, *Chem. Soc. Rev.*, 2019, **48**, 3193–3228.

4   J. A. Martens, A. Bogaerts, N. De Kimpe, P. A. Jacobs, G. B. Marin, K. Rabaey, M. Saeys and S. Verhelst, *ChemSusChem*, 2017, **10**, 1039–1055.

5   K. Müller, L. Mokrushina and W. Arlt, *Chem. Ing. Tech. (Weinh)*, 2014, **86**, 497–503.

6   Y. Yang and J. W. Lee, *Chem. Sci.*, 2019, **10**, 3905–3926.

7   Q. Liu, L. Wu, R. Jackstell and M. Beller, *Nat. Commun.*, 2015, **6**, 1–15.

8   Z. Wang, H. Song, H. Liu and J. Ye, *Angew. Chem. Int. Ed.*, 2020, **59**, 8016–8035.

9   V. Kumaravel, J. Bartlett and S. C. Pillai, *ACS Energy Lett.*, 2020, **5**, 486–519.

10   A. Gautham, D. Baby, P. V. Sreedevi, P. M. Ismail and T. Babitha, *Int. J. Adv. Res.*, 2020, **8**, 1300–1305.

11   T. Niemi and T. Repo, *Eur. J. Org. Chem.*, 2019, 1180–1188.

12   P. Brunel, J. Monot, C. E. Kefalidis, L. Maron, B. Martin-Vaca and D. Bourissou, *ACS Catal.*, 2017, **7**, 2652–2660.

13   X. Liu, M.-Y. Wang, S.-Y. Wang, Q. Wang and L.-N. He, *ChemSusChem*, 2017, **10**, 1210–1216.

14   M. Y. Wang, Q. W. Song, R. Ma, J. N. Xie and L. N. He, *Green Chem.*, 2015, **18**, 282–287.

15   F. Della Monica, A. Buonerba and C. Capacchione, *Adv. Synth. Catal.*, 2019, **361**, 265–282.

16   G.-M. Liang, P. Xiong, K. Azam, Q.-L. Ni, J.-Q. Zeng, L.-C. Gui and X.-J. Wang, *Inorg. Chem.*, 2020, **59**, 1653–1659.

17   F. M. Al-Qaisi, A. K. Qaroush, A. H. Smadi, F. Alsoubani, K. I. Assaf, T. Repo and A. F. Eftaiha, *Dalton Trans.*, 2020, **49**, 7673–7679.

18   X. Wang, W. Y. Gao, Z. Niu, L. Wojtas, J. A. Perman, Y. S. Chen, Z. Li, B. Aguila and S.

Ma, *ChemComm.*, 2018, **54**, 1170–1173.

19   P. Sonzini, C. Damiano, D. Intrieri, G. Manca and E. Gallo, *Adv. Synth. Catal.*, 2020, **362**, 2961–2969.

20   Y. Xie, C. Lu, B. Zhao, Q. Wang and Y. Yao, *J. Org. Chem.*, 2019, **84**, 1951–1958.

21   S. Arshadi, A. Banaei, S. Ebrahimiasl, A. Monfared and E. Vessally, *RSC Adv.*, 2019, **9**, 19465–19482.

22   A. H. Liu, Y. L. Dang, H. Zhou, J. J. Zhang and X. B. Lu, *ChemCatChem*, 2018, **10**, 2686–2692.

23   V. B. Saptal and B. M. Bhanage, *ChemSusChem*, 2016, **9**, 1980–1985.

24   Y. Wu and G. Liu, *Tetrahedron Lett.*, 2011, **52**, 6450–6452.

25   Z. Z. Yang, Y. N. Li, Y. Y. Wei and L. N. He, *Green Chem.*, 2011, **13**, 2351–2353.

26   Z.-Z. Yang, L.-N. He, S.-Y. Peng and A.-H. Liu, *Green Chem.*, 2010, **12**, 1850–1854.

27   M. Sengoden, M. North and A. Whitwood, *ChemSusChem*, 2019, **12**, 3296–3303.

28   F. Zhou, S. L. Xie, X. T. Gao, R. Zhang, C. H. Wang, G. Q. Yin and J. Zhou, *Green Chem.*, 2017, **19**, 3908–3915.

29   C. S. Cao, Y. Shi, H. Xu and B. Zhao, *Dalton Trans.*, 2018, **47**, 4545–4553.

30   S. Arayachukiat, P. Yingcharoen, S. V. C. Vummaleti, L. Cavallo, A. Poater and V. D. Elia, *Mol. Catal.*, 2017, **443**, 280–285.

31   D. Carminati, E. Gallo, C. Damiano, A. Caselli and D. Intrieri, *Eur. J. Inorg. Chem.*, 2018, **2018**, 5258–5262.

32   Y. Chen, R. Luo, Z. Yang, X. Zhou and H. Ji, *Sustain. Energy Fuels*, 2018, **2**, 125–132.

33   Y. Lee, J. Choi and H. Kim, *Org. Lett.*, 2018, **20**, 5036–5039.

34   G. Bresciani, L. Biancalana, G. Pampaloni and F. Marchetti, *Molecules*, 2020, **25**, 3603.

35   D. B. Dell'Amico, F. Calderazzo, L. Labella, F. Marchetti and G. Pampaloni, *Chem. Rev.*, 2003, **103**, 3857–3898.

36   L. Biancalana, G. Bresciani, C. Chiappe, F. Marchetti, G. Pampaloni and C. S. Pomelli, *Phys.*

Chem. Chem. Phys., 2018, **20**, 5057–5066.

37   L. Biancalana, G. Pampaloni, S. Zacchini and F. Marchetti, *J. Organomet. Chem.*, 2018, **869**, 201–211.

38   M. H. Chisholm and M. W. Extine, *J. Am. Chem. Soc.*, 1977, **99**, 792–802.

39   G. Bresciani, M. Bortoluzzi, F. Marchetti and G. Pampaloni, *ChemSusChem*, 2018, **11**, 2737–2743.

40   G. Bresciani, F. Marchetti and G. Pampaloni, *New J. Chem.*, 2019, **43**, 10821–10825.

41   G. Pampaloni, G. Bresciani, M. Bortoluzzi, C. Ghelarducci and F. Marchetti, *New J. Chem.*, 2021, DOI:10.1039/D0NJ05657J.

42   G. Bresciani, F. Marchetti, G. Rizzi, A. Gabbani, F. Pineider and G. Pampaloni, *J. CO2 Util.*, 2018, **28**, 168–173.

43   C. Forte, M. Hayatifar, G. Pampaloni, A. M. R. Galletti, F. Renili and S. Zacchini, *J. Polym. Sci. Part A Polym. Chem.*, 2011, **49**, 3338–3345.

44   M. Bortoluzzi, G. Bresciani, F. Marchetti, G. Pampaloni and S. Zacchini, *New J. Chem.*, 2017, **41**, 1781–1789.

45   G. Bresciani, M. Bortoluzzi, S. Zacchini, F. Marchetti and G. Pampaloni, *Eur. J. Inorg. Chem.*, 2018, **2018**, 999–1006.

46   M. H. Chisholm and M. W. Extine, *J. Am. Chem. Soc.*, 1977, **99**, 782–792.

47   M. Bortoluzzi, E. Ferretti, F. Marchetti, G. Pampaloni and S. Zacchini, *Dalton Trans.*, 2016, **45**, 6939–6948.

48   M. Jura, W. Levason, R. Ratnani, G. Reid and M. Webster, *Dalton Trans.*, 2010, **39**, 883–891.

49   J. A. M. Canich and F. A. Cotton, *Inorganica Chim. Acta*, 1989, **159**, 163–168.

50   R. A. Henderson, D. L. Hughes and A. N. Stephens, *J. Chem. Soc., Dalt. Trans.*, 1990, 1097.

51   P. Trinchera, B. Musio, L. Degennaro, A. Moliterni, A. Falcicchio and R. Luisi, *Org. Biomol. Chem.*, 2012, **10**, 1962–1965.

52   D. J. Darensbourg, J. R. Andreatta and A. I. Moncada, in *Carbon Dioxide as Chemical Feedstock*, Wiley-VCH Verlag GmbH & Co. KGaA, Weinheim, Germany, pp. 213–248.

53   N. Bartalucci, F. Marchetti, S. Zacchini and G. Pampaloni, *Dalton Trans.*, 2019, **48**, 5725–5734.

54   F. Calderazzo, P. Pallavicini, G. Pampaloni and P. F. Zanazzi, *J. Chem. Soc., Dalt. Trans.*, 1990, 2743.

55   X. Kang, L. Yao, Z. Jiao and B. Zhao, *Chem. – An Asian J.*, 2019, **14**, 3668–3674.

56   S. Carrasco, A. Sanz-Marco and B. Martín-Matute, *Organometallics*, 2019, **38**, 3429–3435.

57   G. Bresciani, M. Bortoluzzi, S. Zacchini, A. Gabbani, F. Pineider, F. Marchetti and G. Pampaloni, *Eur. J. Inorg. Chem.*, 2018, **2018**, 1176–1184.

58   F. Calderazzo, S. Ianelli, G. Pampaloni, G. Pelizzi and M. Sperrle, *J. Chem. Soc., Dalt. Trans.*, 1991, 693.

59   P. B. Arimondo, F. Calderazzo, U. Englert, C. Maichle-Mössmer, G. Pampaloni and J. Strähle, *J. Chem. Soc., Dalt. Trans.*, 1996, 311–319.

60   M. Bortoluzzi, F. Ghini, M. Hayatifar, F. Marchetti, G. Pampaloni and S. Zacchini, *Eur. J. Inorg. Chem.*, 2013, 3112–3118.

61   D. Belli Dell'Amico, L. Labella, F. Marchetti, P. Mastrorilli, S. Samaritani and S. Todisco, *Polyhedron*, 2013, **65**, 275–281.

62   D. Belli, D. Amico, D. Boschi, F. Calderazzo, S. Ianelli, L. Labella, F. Marchetti, G. Pelizzi, E. Guy and F. Quadrelli, *Inorganica Chim. Acta*, 2000, **302**, 882–891.

63   D. Belli Dell'Amico, F. Calderazzo, B. Giovannitti and G. Pelizzi, *J. Chem. Soc., Dalt. Trans.*, 1984, 647–652.

64   E. Agostinelli, D. Belli Dell'Amico, F. Calderazzo, D. Fiorani and G. Pelizzi, *Gazz. Chim. Ital.*, 1988, **188**, 729–740.

65   R. Alessio, D. B. Dell'Amico, F. Calderazzo, U. Englert, A. Guarini, L. Labella and P. Strasser, *Helv. Chim. Acta*, 1998, **81**, 219–230.

66   D. Belli Dell'Amico, F. Calderazzo, M. Dell'Innocenti, B. Güldenpfennig, S. Ianelli, G. Pelizzi and P. Robino, *Gazz. Chim. Ital.*, 1993, **123**, 283–288.

67   L. Abis, D. B. Dell'Amico, F. Calderazzo, R. Caminiti, F. Garbassi, S. Ianelli, G. Pelizzi, P. Robino and A. Tomei, *J. Mol. Catal. A Chem.*, 1996, **108**, L113–L117.

68   G. R. Fulmer, A. J. M. Miller, N. H. Sherden, H. E. Gottlieb, A. Nudelman, B. M. Stoltz, J. E. Bercaw and K. I. Goldberg, *Organometallics*, 2010, **29**, 2176–2179.

69   D. A. Skoog, D. M. West and F. J. Holler, in *Fundamentals of Analytical Chemistry*, Thomson Learning, Inc., Stamford, Connecticut, USA, 7th edn., 1996.

70   G. M. Sheldrick, SADABS-2008/1 - Bruker AXS Area Detector Scaling and Absorption Correction, Bruker AXS, Madison, Wisconsin, USA, 2008.

71   G. M. Sheldrick, *Acta Crystallogr. Sect. A Found. Crystallogr.*, 2015, **71**, 3–8.

72   H. D. Flack, *Acta Crystallogr. Sect. A Found. Crystallogr.*, 1983, **39**, 876–881.

73   G. Bresciani, E. Antico, G. Ciancaleoni, S. Zacchini, G. Pampaloni and F. Marchetti, *ChemSusChem*, 2020, **13**, 5586-5594.